Astron. Astrophys. 351, 133–139 (1999)

ASTRONOMY AND ASTROPHYSICS

Magnetic field and radial velocity of the CP2 star α^2 CVn*

E. Gerth[1], **Yu.V. Glagolevskij**[2], **G. Hildebrandt**[1], **H. Lehmann**[3], **and G. Scholz**[1]

[1] Astrophysikalisches Institut Potsdam, Telegrafenberg A 27, 14473 Potsdam, Germany (0331973826@t-online.de; ghildebrandt, gscholz@aip.de)
[2] Special Astrophysical Observatory of Russian AS, Nizhnij Arkhyz 357147, Russia (glagol@relay.sao.ru)
[3] Thüringer Landessternwarte Tautenburg, Karl-Schwarzschild-Observatorium, 07778 Tautenburg, Germany (lehm@tls-tautenburg.de)

Received 3 February 1999 / Accepted 19 April 1999

Abstract. We analyse spectra of the well-known bright CP2 star α^2 CVn in order to test the suitability of a new equipment for magnetic field observations and a computer program for the calculation of magnetic surface maps.

The variation of the longitudinal magnetic field, derived from the elements H and Si II, which are distributed probably homogeneously on the stellar surface, can be represented by the superposition of a dipole with a quadrupole using the model of the oblique rotator. The corresponding magnetic field structure on the stellar surface is compared with the distributions of the chemical elements Ti, Cr, and Fe determined by several authors.

A series of CCD coudé spectra as well as some selected observational sets, obtained by other authors in the last decades, were used for the search for periods in radial velocities. The accuracy of the period derived for a single data set does not allow us to draw a conclusion on the existence of a phase shift between the data sets.

Key words: stars: chemically peculiar – stars: individual: α^2 CVn – stars: magnetic fields – stars: rotation

1. Introduction

HD 112413 = α^2 CVn is a CP2 star whose outstanding variability in line intensities and radial velocities (hereinafter RV) has been known for a very long time. Since the beginning of this century several authors have devoted much effort to the description of the extraordinary changes of the RVs (Ludendorff, (1906)) and of the line intensities (Belopolsky, (1914)). The line intensity variations could be represented with a period of about $5\overset{\mathrm{d}}{.}5$. The later investigations of the RVs by Farnsworth (1932), and mainly the detailed study by Struve & Swings (1943) and by Pyper (1969) confirmed the spectral variability and showed additionally that the amplitudes and the shape of the radial velocity curves of the various elements implies a classification in three groups having the same value of the mean velocity. In Struve & Swings's first group (a), including the velocity variations of the rare earths elements and of Ca I, Mn I, and Ni I, the amplitude in velocity is more than 10 km s^{-1}. Their second group (b) contains the elements Fe, Cr, Mn II, and Ti, which show more or less markedly a double wave in the velocity variation as well as a distinctly smaller range in the amplitude, and finally, in the third group (c) the elements Si II, Mg II, Ca II, and H show no distinct variability.

In the early fifties α^2 CVn was one of the first peculiar stars in which the behaviour of a magnetic field was investigated. In the following we will distinguish between the component of the magnetic field in the line of sight, i.e. the longitudinal or effective magnetic field (hereinafter $B_{\rm eff}$) and the mean surface field (hereinafter $B_{\rm s}$). The observations of $B_{\rm eff}$ by Babcock & Burd (1952), Pyper (1969), and Oetken et al. (1970), based on photographic plates, gave altogether a very anharmonic $B_{\rm eff}$ curve. Moreover, the individual spectral lines and elements show a very large diversity of the form and amplitude with the same period derived from the intensity and velocity variations. Later photoelectric observations of $B_{\rm eff}$ by Borra & Landstreet (1977), obtained using a hydrogen-line magnetograph, give values of the magnetic field strength in the approximate limits of about +1500 gauss and −1500 gauss. The magnetic curve does not show the strong anharmonic shape as known from the photographic measurements. The difference between the magnetic curves seems to be partially caused by the measuring process. However, the contribution of a nonuniform distribution of the chemical elements on the stellar surface has an influence on the magnetic curve. This is clearly seen from the anharmonic magnetic curve of $B_{\rm eff}$, derived by Borra & Vaughan (1978) from photoelectric measurements of the Fe II-line 4520.2 Å. Owing to the broad spectral lines, the surface field $B_{\rm s}$ is difficult to measure and not known yet.

It was shown, e.g. by Michaud (1970) and Glagolevskij (1994), that the distribution of the chemical elements on the surface of magnetic early-type stars is connected with the magnetic field. Therefore, it is appropriate to look for a relation between the observed concentration of chemical elements and the magnetic field configuration.

Considering the time interval of about 90 years between Ludendorff's first RV observations and the recent ones, it could

Send offprint requests to: G. Scholz

* Based on spectroscopic observations taken with the 2 m telescope at the Thüringer Landessternwarte Tautenburg, Germany.

Table 1. Spectroscopic parameters.

spectral region in Å	dispersion in Å/pixel	resolving power	mean S/N
TRAFICOS			
5000–6700	0.06	25800	70
COUDÉ			
4800–7200	0.08	37000	250

be also useful to investigate the relation of suitable data sets and their temporal behaviour.

2. Observations and reductions

Our spectroscopic observations were performed with the 2 m telescope of the Thüringer Landessternwarte Tautenburg using two different spectrographs: on the one hand, the échelle spectrograph and Zeeman analyzer attached at the Nasmyth focus (TRAFICOS, Hildebrandt et al. (1997)), on the other hand, the échelle coudé spectrograph. $B_{\rm eff}$ and RV values have been calculated using specially developed reduction programs under MIDAS. Table 1 lists the parameters of the spectra obtained. In order to take into account the strong line intensity variations, we have separated the RVs and the $B_{\rm eff}$ values in two groups. The first group comprises the elements Cr and Fe and the second group contains the elements H and Si. All in all RVs were determined from 25 lines of Fe II, 9 lines of Cr II, 4 lines of Si II, and from H_α. Line positions of metal lines have been determined by simple gaussian fits. For H_α we used a sum of one Lorentz and two gaussian functions to fit the line profile. Telluric lines have been removed by an iterative procedure.

3. Radial velocities

The RVs, calculated from our spectra, are listed in Table 2. The phases follow from the ephemeris derived from the intensity variations of the Eu II line by Farnsworth:

$$\mathrm{JD} = 2419869.720 + 5\overset{\mathrm{d}}{.}46939\mathrm{E}\ .$$

In the past all investigations, concerning the temporal behaviour of the RVs, presupposed the astonishingly accurate indicated period of $5\overset{\mathrm{d}}{.}46939$ determined from intensity variations. Because RVs of α^2 CVn are known since the beginning of the century it is certainly worth to investigate some suitable RV data sets on their periodic behaviour. The very first RVs come from 12 Potsdam spectrograms obtained between March 1901 and May 1905 and notified by Ludendorff (1906). Another set of RVs contains 32 RVs published by Farnsworth (1932). In both data sets the RVs are means from different metallic lines. A further set contains the RVs of the rare earths and Ti, Cr, and Fe in the above mentioned paper of Struve & Swings (1943) and another one the RVs derived of the same elements by Pyper (1969). Finally, we assigned the RVs of Cr and Fe as well as of H and Si of Table 2 to the set (5). We consider all sets to be on the IAU RV standard. (In order to reduce Ludendorff's RVs to the IAU standard we have added a correction of -0.3 km s^{-1} to all measured RVs, Scholz et al. (1997a)).

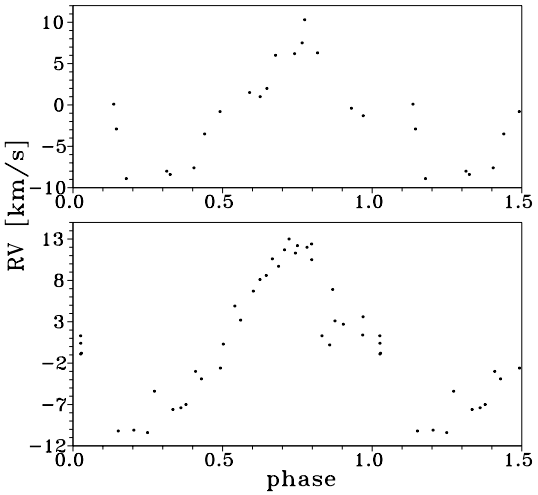

Fig. 1. Variation of the radial velocity for rare earths, folded with the common period of $5\overset{\mathrm{d}}{.}46939$. *Top:* data set 3, *bottom:* data set 4.

3.1. Period search

For the period search we assumed a ground wave and its first harmonic. Details of the period search technique used are described in Lehmann et al. (1995). The results are listed in Table 3. For every data set and for the different elements, excepted for H_α and Si II, we found the most significant peak in the Scargle periodogram either near to the value of $5\overset{\mathrm{d}}{.}47$ or near to $2\overset{\mathrm{d}}{.}735$, the last one mainly for the RVs given by Ludendorff and Farnsworth. These periods correspond to $P_{\rm Eu\,II} = 5\overset{\mathrm{d}}{.}46939$, given by Farnsworth for the intensity variation of the Eu II lines, and to its first harmonic, respectively. The accuracy of the periods found and the very long time interval between the first and last recorded RV measurements does not allow the determination of a common period because we cannot exclude a remarkable phase shift between them. Therefore, we assume for all data sets the common period of $P_{\rm Eu\,II}$. If this value were accurate up to 10^{-5} d, the remaining error would introduce a phase shift between the data of Struve & Swings (set 3) and our data (set 5) of 0.04, and for a phase shift of 0.1 we get an accuracy limit of the period of $2.5\,10^{-4}$ d.

For the further discussion we exclude the RVs given by Ludendorff and Farnsworth. Both data sets show a large scattering and do not have a specification after elements. So we consider only the data sets (3), (4), and (5).

As is mentioned above, we can distinguish between several groups of chemical elements which show different behaviour in radial velocity variation. We have not determined RVs of rare earths, but it seems to be justified to investigate the RVs of these elements which have the largest RV variation. Fig. 1 shows the phase diagrams of the RV values for rare earths given by Struve & Swings and Pyper with the period of $P_{\rm Eu\,II}$. The variation of the two data sets agrees very well in phase. Although some

Table 2. Mean RVs of individual elements derived from Tautenburg spectra. The phases are calculated with the ephemeris given by Farnsworth (1932).

HJD 2 400 000+	RV H_α (km s^{-1})	RV Si II (km s^{-1})	RV Cr II (km s^{-1})	RV Fe II (km s^{-1})	phase
50652.3422	-4.92 ± 0.23	-1.02 ± 1.33	-4.75 ± 0.72	-3.70 ± 0.45	0.164
50656.3722	-3.73 ± 0.23	-2.99 ± 0.81	$+8.34 \pm 0.69$	$+3.51 \pm 0.63$	0.901
50656.3785	-3.77 ± 0.31	-2.82 ± 1.02	$+8.75 \pm 0.77$	$+3.54 \pm 0.59$	0.902
50708.2691	-4.04 ± 0.19	-1.36 ± 1.29	$+2.91 \pm 1.55$	-3.27 ± 0.40	0.389
50708.2763	-4.09 ± 0.19	-1.39 ± 1.29	$+3.77 \pm 1.51$	-3.24 ± 0.42	0.390
50709.2652	-1.80 ± 0.27	-1.66 ± 1.00	-6.41 ± 1.27	-1.82 ± 0.52	0.571
50709.2719	-1.51 ± 0.30	-1.38 ± 1.17	-6.00 ± 1.31	-1.89 ± 0.55	0.572
50710.2643	-3.64 ± 0.24	-1.40 ± 0.77	-0.79 ± 1.10	-2.50 ± 0.46	0.754
50712.2705	-4.30 ± 0.22	-0.91 ± 1.14	-8.45 ± 0.50	-6.36 ± 0.58	0.121
50713.2734	-3.16 ± 0.19	-1.03 ± 0.50	-0.19 ± 0.94	-3.49 ± 0.48	0.304
50714.2687	-1.32 ± 0.20	-2.08 ± 0.98	-5.18 ± 0.29	-3.18 ± 0.51	0.486
50848.6421	-2.61 ± 0.11	-1.07 ± 0.69	-6.05 ± 0.61	-2.80 ± 0.49	0.054
50863.5616	-2.19 ± 0.19	-0.19 ± 0.60	$+3.68 \pm 0.40$	$+0.02 \pm 0.43$	0.782
50884.4180	-2.13 ± 0.20	-0.44 ± 0.89	-3.45 ± 0.33	-1.56 ± 0.42	0.595
50918.3916	-2.19 ± 0.15	-0.10 ± 0.92	$+5.10 \pm 0.45$	$+1.15 \pm 0.42$	0.807
50942.5921	-2.44 ± 0.16	-2.04 ± 1.09	-2.08 ± 0.80	-3.28 ± 0.50	0.232
50942.5969	-2.47 ± 0.16	-1.65 ± 0.84	-2.07 ± 0.80	-3.09 ± 0.52	0.233
50967.3477	-2.05 ± 0.20	-2.05 ± 1.06	$+0.75 \pm 0.70$	-1.90 ± 0.57	0.758
50967.3537	-1.87 ± 0.21	-1.96 ± 1.08	$+0.77 \pm 0.70$	-1.86 ± 0.59	0.759
50973.5220	-1.98 ± 0.18	-2.47 ± 1.13	$+6.34 \pm 0.62$	$+2.24 \pm 0.56$	0.887
50973.5288	-1.92 ± 0.18	-2.38 ± 1.05	$+6.62 \pm 0.62$	$+2.30 \pm 0.54$	0.888
51009.3551	-2.01 ± 0.22	-2.73 ± 1.95	$+7.51 \pm 1.80$	-1.71 ± 0.53	0.438
51010.3593	-1.40 ± 0.17	-1.39 ± 0.92	-3.62 ± 0.85	-2.50 ± 0.46	0.622
51010.3645	-1.44 ± 0.17	-1.28 ± 0.89	-3.20 ± 0.70	-2.62 ± 0.42	0.623

structures can be seen in the phase diagrams, there is no hint of the existence of secondary maxima.

Another group that we investigated contains the elements Ti II, Cr I, Cr II, Fe I, and Fe II. This group, represented mainly by Cr II, shows velocity-curves with a double wave, for the different elements the maxima and minima are more or less in phase. The results of our period search are represented in Fig. 2 and Table 3. Besides differences in the absolute amplitude of the variation differences exist also in the ratio of the amplitudes of the ground wave and its first harmonic (columns A_0/A_1, C_0/C_1). The two upper panels of Fig. 2 represent the phase diagrams of the RV means of these elements given by Struve & Swings and by Pyper, respectively, and the following two panels show the RVs for Cr II and Fe II of Table 2.

In comparison with the RV curves of Fig. 1 the amplitude of the variation is smaller and the frequency is doubled, the amplitude of the first harmonic dominates the variation. Our measurements show a much larger amplitude of the variation for Cr II than for Fe II and similar to the finding notified by Struve & Swings, the double-wave character of the variation is much more prominent for Cr II than for Fe II. Furthermore, whereas the variation of the RVs derived from our observations is well positioned in phase with the observation by Struve & Swings, the data by Pyper are almost in anti-phase. From the limits in phase accuracy estimated above it is clear that the large phase shift observed for the values by Pyper cannot be explained by an uncertainty in the period assumed. But, Pyper derived four branches of the RV curve of the iron-peak elements during

Table 3. Results of period search. For each data set we give the elements used by the different authors for the RV determination, the derived period in days, and the half-amplitudes A_0, A_1 in km s^{-1} for this period and its first harmonic, respectively. C_0 and C_1 are the half-amplitudes obtained by assuming a common period of $5\overset{\mathrm{d}}{.}46939$. RV_m gives the time averaged mean value of RV.

data set	*lines*	P	A_0	A_1	C_0	C_1	RV_m
1	mix	5.4779	2.2	2.0	1.0	1.7	± 0.0
2	mix	5.7470	0.4	3.0	1.6	0.8	-0.8
3	Fe I/Fe II Cr I/Cr II Ti II	5.4690	0.4	3.6	0.7	3.9	-0.2
	rare earths	5.4675	7.3	1.1	6.7	1.2	-0.9
4	Fe I/Fe II Cr I/Cr II Ti II	5.4727	1.4	2.8	0.9	2.3	-2.1
	rare earths	5.4706	10.1	0.7	9.5	1.3	$+0.5$
5	Cr II	5.4684	1.9	5.4	1.8	5.6	-0.2
	Fe II	5.4775	3.1	1.4	2.3	1.8	-1.6
	Si II	–	–	–	(0.4)	–	-1.6
	H_α	–	–	–	(1.0)	–	-2.6

data sets are: 1 Ludendorff JD 2415470...2416994
2 Farnsworth JD 2426355...2426529
3 Struve & Swings JD 2429031...2430151
4 Pyper JD 2438837...2439343
5 our data JD 2450652...2451010

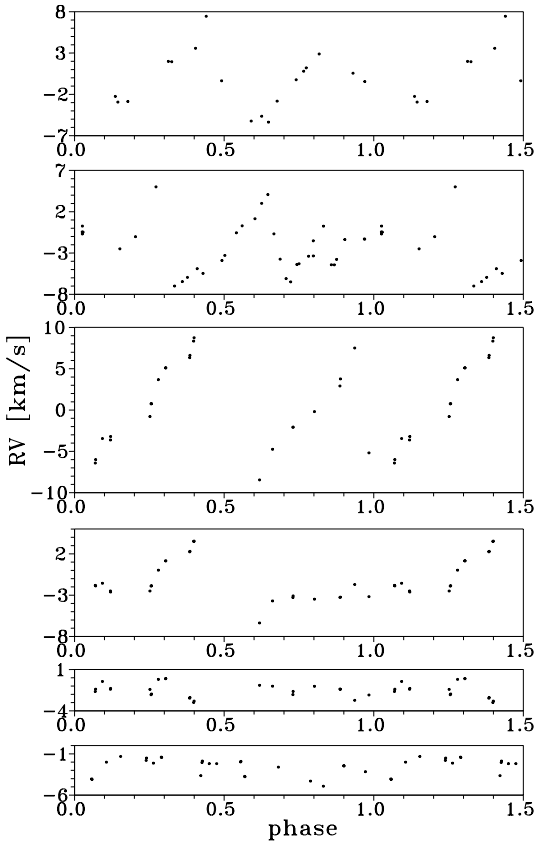

Fig. 2. Radial velocity variation of different elements, folded with the common period of $5^{\rm d}.46939$. The different panels correspond to the following elements and data sets: *First panel:* data set 3 of Ti II, Cr I, Cr II, Fe I, Fe II; *second panel:* data set 4 (elements as before); *third panel:* data set 5 of Cr II; *fourth panel:* data set 5 of Fe II; *fifth panel:* data set of Si II; *sixth panel:* data set 5 of H_α.

one cycle. Therefore, the use of different samples of spectral lines can produce different phase shifts in the RV diagrams, as is observed in the present case. Accordingly, in looking for certain trends in RVs the behaviour of every element has to be separately considered.

Finally, the lines of Si II and the Balmer line H_α show no significant changes in RV, to see in the last two panels of Fig. 2.

4. Aspect angle and stellar parameters

First we determine the aspect angle i which is the inclination between the rotation axis and the line of sight. To estimate the angle i we go out from $v{\cdot}\sin i$. It seems that the most correct value is given in the paper by Khokhlova & Pavlova (1984) with $v{\cdot}\sin i = 17\,\mathrm{km\,s^{-1}}$ and an error smaller than 10%. Assuming the effective temperature of the star to be $T_{\rm eff}$ = 11120 K (Glagolevskij, 1994) and a H_β-Index of 2.777, (Rufener, 1981), the absolute bolometric magnitude $M_{\rm bol} = -0.28$ follows. By using the radiation law the radius can be derived from

$$\log R/R_\odot = 8.46 - 2\log T_{\rm eff} - 0.2 M_{\rm bol}$$

with $M_{\rm bol}$ in mag and $T_{\rm eff}$ in K. We get $2.6 R_\odot$ for the radius of α^2 CVn.

Table 4. $B_{\rm eff}$ values for individual elements. The phases are calculated with the ephemeris of Farnsworth, n is the number of the lines measured.

HJD 2450000+	$B_{\rm eff}$(Cr/Fe) (gauss)	n	$B_{\rm eff}$(H/Si II) (gauss)	n	phase
494.658	$+860 \pm 280$	9	$+340 \pm 340$	4	0.333
496.646	-910 ± 350	6	-900	1	0.697
528.513	$+1150 \pm 290$	8	$+1110 \pm 170$	2	0.523
556.427	-390 ± 130	7	-400 ± 410	3	0.627
558.420	-920 ± 180	6	-740 ± 300	3	0.991
559.455	-560 ± 130	10	-560 ± 340	5	0.180
583.378	$+560 \pm 440$	7	$+900 \pm 190$	4	0.555
585.347	-960 ± 220	4	-1080 ± 330	4	0.914
586.391	-970 ± 230	11	-800 ± 280	5	0.105
588.364	$+1480 \pm 440$	8	$+980 \pm 180$	3	0.466

For an oblique rotator, the equatorial rotational velocity v, the period P, and the stellar radius R are related by

$$v = 50.6 R/P$$

if R, v, and P are expressed in solar radii, $\mathrm{km\,s^{-1}}$, and days, respectively. With $P = 5^{\rm d}.46939$ we have $i = 45°$ resp. 135°. (We mention that the calculations made by Pyper and by Oetken give $i = 50°$).

5. Magnetic field

5.1. Magnetic field observations

For the investigation of the magnetic field of α^2 CVn we exclude the photographic determined $B_{\rm eff}$ values given by Pyper and Oetken, which show a very anharmonic variation, quite different for the various elements. The results have been discussed by Oetken (1979) in detail.

Considering the accuracy of the $B_{\rm eff}$ values listed in Table 4, no significant differences can be established between the data derived for the individual elements. Nevertheless, for the further analysis we use only the values determined for the H- and Si II-lines and the data given by Borra & Landstreet (1977) for the H-lines which agree quite well with each other. Because the RVs of these elements do not show remarkable variations, a homogeneous distribution of the elements on the stellar surface could be assumed. In Fig. 3 the $B_{\rm eff}$ values are represented folded with the period given by Farnsworth.

5.2. Magnetic maps

The basic ideas for the calculation of the magnetic surface map have been already described by Gerth et al. (1997, 1998) and some first results have been published for γ Equ (Scholz et al. 1997b) or CU Vir (Glagolevskij et al. 1998). A detailed description of all procedures is in preparation by Gerth & Glagolevskij so that we will here make only a few remarks.

The distribution of the magnetic field on the stellar surface is calculated by matrices in which the elements are defined by the spherical coordinates of the longitude and the latitude. The

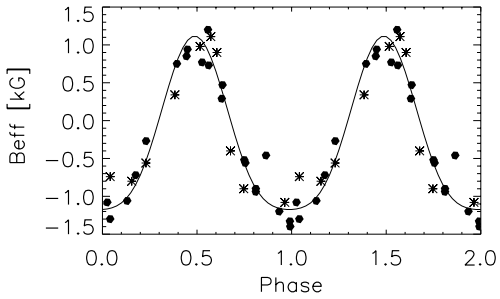

Fig. 3. $B_{\rm eff}$ values derived from the H line by Borra & Landstreet (points) and the H/Si II lines of the TRAFICOS observations (asterisks). The curve represents the longitudinal magnetic field following from our dipole-quadrupole model.

Table 5. Pole field strengths $B_{\rm p}$ on the stellar surface and positions of the 'magnetic quantities' in α^2 CVn.

$B_{\rm p}$ (kG)	longitude (°)	latitude (°)
dipole		
+8.96	90	3
−8.96	270	−3
quadrupole		
−5.98	0	0
5.98	90	3
−5.98	180	0
5.98	270	−3

magnetic field vector consists of three components with unity vectors spanned in the direction of the stellar radius (normal vector), in direction of the longitude (φ-vector) and in direction of the latitude (δ-vector). Assuming point-like field sources in the interior of the star the potential is simply the linear superposition of the potentials of the single field sources for which the potential can be calculated. Then the field vector is easily derived by the gradient of the potential. In order to consider the aspect of the different visibility of the hemisphere, the program computes for any inclination angle with respect to the rotation axis the projection of the elements and the limb darkening, storing them into a rectangular matrix of the same rank as the map. The matrices of the map and of the 'aspect window' are now subjected to a matrix convolution for the determination of the map of the magnetic field distribution, expressed in a cylindrical projection at the stellar surface.

5.3. Dipole field

The magnetic field values of α^2 CVn show the frequently observed fact of many other magnetic CP stars, that one extremum of the $B_{\rm eff}$ curve is stronger and broader than the other one. This appearance requires a field geometry which differs from that of the simple centered dipole. In their investigation Borra & Landstreet were able to fit very satisfactorily the $B_{\rm eff}$ curve by a set of moderately decentered-dipole models. Another possibility to explain the observations will be discussed in the next paragraph.

5.4. Dipole-quadrupole field

For the analysis the following notation and assumptions have been adopted:

- i, angle between the rotation axis and the line of sight,
- β, angle between the rotation axis and the magnetic axis, and furthermore,
- the variation of $B_{\rm eff}$ is produced by the superposition of a dipole and an axisymmetrical quadrupole lying in the equatorial plane. For the angle i the value determined in Sect. 4 is assumed, the angle β follows from the fit procedure. Such a model is another possible suggestion to represent the distribution of the magnetic field on the stellar surface. For the magnetic field variation of α^2CVn Pyper already assumed a combination of dipole and quadrupole fields, whose axes approximately coincide and are inclined by an angle of about 50° to the axis of rotation. This field is symmetrical about the meridian that passes through the rotational pole and the magnetic poles, but is not symmetrical about the magnetic equator. Later Oetken (1977) discussed in detail the consequences of a dipole-quadrupole combination in her equatorially symmetric rotator model. In this model the dipole and quadrupole are lying in the equatorial plane with their axes in the same direction.

Assuming such a model the result of our calculations for α^2 CVn is summarized in Table 5 and represented in Fig. 3 by the solid curve. The best fit includes the combination of the angles i = 135° and β = 87°. With β = 87° the geometry of our model is a little different from that presupposed by Oetken (equatorial plane exactly). The 'magnetic quantities' are located at the distance of r = 0.15 from the centre and yield the magnetic pole field strengths on the stellar surface given in the first column of Table 5. The parameter r has been found by modeling of the effective field $B_{\rm eff}$ and surface field $B_{\rm s}$ of other magnetic CP stars investigated. In all cases we found that the results of the modeling show only a very small dependence upon the value of r.

5.5. Average surface magnetic field

In Fig. 4 the calculated variation of the average surface magnetic field $B_{\rm s}$ is shown according to the supposed dipole-quadrupole model parameters of Table 5. Unfortunately, the broad spectral lines do not allow one to measure $B_{\rm s}$ and to determine the variability with the rotational period as it was done for many other magnetic CP stars in the commendable investigation by Mathys et al. (1997) so that a further improvement of the model parameters is not possible.

6. Magnetic field structure and element distribution

The relation between the distribution of the magnetic field and the chemical element concentration has a basic significance for the diffusion theory. To search for a relation we compare

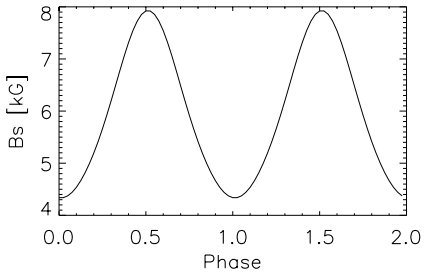

Fig. 4. Calculated average surface magnetic field following from our dipole-quadrupole model.

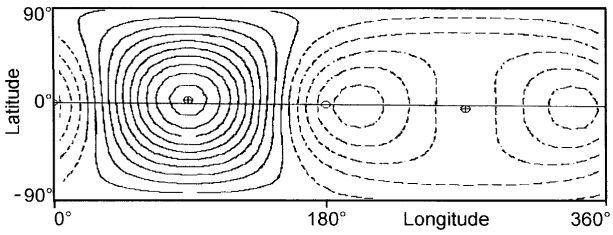

Fig. 5. Cylindrical projection of the magnetic field distribution at the stellar surface. The full lines correspond to the positive field and the dashed lines the negative field of the dipole-quadrupole model.

the calculated map of the magnetic field distribution ((δ, φ)-vector) corresponding to our dipole-quadrupole structure with the distribution of the chemical elements Fe, Cr, and Ti found by Khokhlova & Pavlova (1984) and Pyper (1969). In Fig. 5 the isoline map of the distribution of the magnetic field is shown and in Fig. 6 the maps of the chemical element distribution are represented. In Fig. 6, the solid lines mark the position of the spots following from the paper by Kokhlova & Pavlova and the dashed lines are those derived by Pyper, respectively. The spots indicated by Pyper combine the iron-peak elements (Ti II, Cr II, Fe II) and do not distinguish between individual elements. The black circles in the panels of Fig. 6 denote the position and the absolute value of the strength of the magnetic poles on the stellar surface (symbolically indicated by the different diameters and the deviation from the equator) corresponding to our model.

The positions of the chemical elements derived by the authors agree only approximately with each other, this holds also for the spots determined by the spectral lines of the same element. Therefore, statements on the relation between the magnetic structure and the element concentration will be quite uncertain.

Considering the maps we see that the chemical elements are concentrated in some regions. In the case of Fe the spots have a large extension in longitude, therefore, a relation to the magnetic field is hard to define. The spots of Ti and Cr, lying in a belt of about $\pm$ 30° along the magnetic equator, seem to coincide in longitude with different magnetic structures. The element Cr coincides obviously more with the positions of the magnetic poles, especially with the areas of the dipole, whereas Ti is located more in the regions of the polarity reversal of the magnetic field. A concentration of individual elements in the areas where the magnetic field changes its polarity could be just

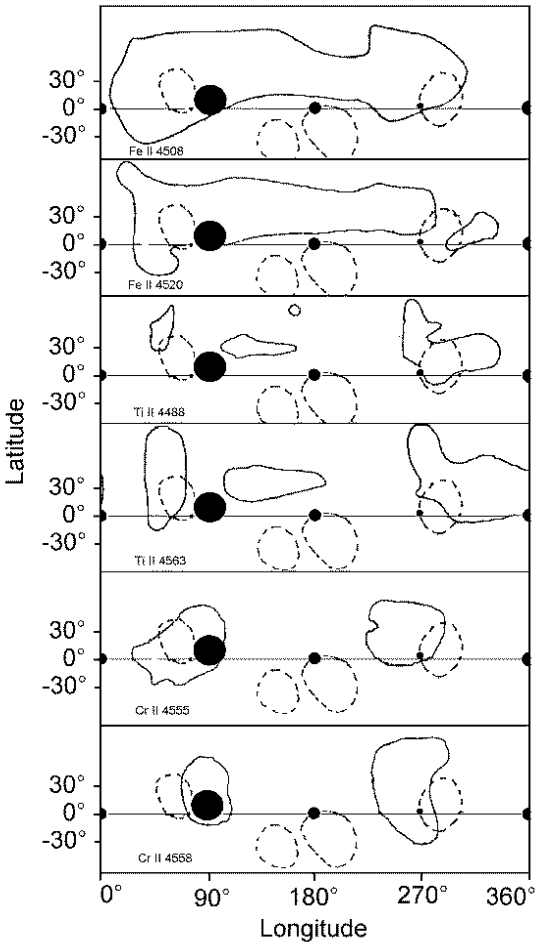

Fig. 6. Element distribution maps of α^2 CVn. The solid lines correspond to the element distribution of Kokhlova & Pavlova (the contours correspond to the curves derived from spectral lines with an equivalent width of about 150 mÅ) and the dashed lines to the distribution of Pyper, respectively.

as well realized as Alécian & Vauclair (1981) and Mégessier (1984) have shown considering the overabundance of Si in Ap stars.

7. Discussion

α^2 CVn is one of the frequently investigated CP stars. The RVs and the equivalent widths of some chemical elements give distinct hints on a very strongly inhomogeneous distribution on the stellar surface. This has to be considered in detailed investigations of the RV and the magnetic field. The nearly constant behaviour of the RVs of the H and the Si II lines as well as the simple shape of their $B_{\rm eff}$(t)-curves are possibly due to a homogeneous distribution of these elements on the stellar surface. Consequently, our investigation of the magnetic field should be more or less representative for the spot-free case. According to our magnetic model the ratio of the quadrupole moment to the dipole moment is 0.66. This value is nearly the same one found in the calculation by Oetken (1979), namely 0.5 in the case of the homogeneous element distribution. Her calculations have

also shown, that with the assumption of an inhomogeneous element distribution the ratio of the quadrupole moment to the dipole moment remarkably increases, namely from 0.5 to 3.2 taking into account the equivalent widths measured. Therefore, in order to study the relation between the magnetic distribution and a concrete element distribution map it is important to know the magnetic curves of the different elements. Though from this point of view the situation is still unsatisfactory, some facts are yet worth to mention:

- the Zeeman échelle spectrograph is suitable for observations of the longitudinal magnetic field as the comparison of Borra & Landstreet's values and our ones shows
- we cannot detect significant variations of the RV of the elements H and Si II. The assumption of a homogeneous surface distribution of these elements should be a quite reasonable one
- the RVs of the elements Cr and Fe vary. Similar to the finding by Struve & Swings, two maxima exist in the phase diagrams folded with the period of the intensity variation, very markedly for Cr but weakly for Fe. Using the ephemeris given by Farnsworth the variations are in phase with the observations by Struve & Swings. The difference to Pyper's result is obviously caused by the use of a different sample of spectral lines of the iron-peak elements. Comparing our RV curves of the elements Fe and Cr with the wide-spreaded Fe and the sharper bounded Cr distribution maps we see that they are quite consistent
- the Fe, Cr, and Ti surface distributions show no unique relation to the calculated magnetic field. The proposed maps allow one to connect the element distribution as well with the areas of the magnetic poles as with the regions where the magnetic field lines have a horizontal direction.

In order to clear present ambiguities, further accurate measurements, suitable to derive simultaneously $B_{\rm eff}$, (and possibly $B_{\rm s}$, too) and the surface element distribution, are necessary for a more reliable study of the relation between the magnetic field and the element concentration.

Acknowledgements. This work was supported by the Thüringer Landessternwarte and its director Prof. J. Solf by allocation of observing time with the échelle spectrograph TRAFICOS. The authors are very grateful to Prof. L. Oetken for her useful suggestions and remarks. Finally, the authors also thank the referee Dr. M. Landolfi for his critical reading of the manuscript and valuable comments.

References

Alécian G., Vauclair S., 1981, A&A 101, 16
Babcock H.W., Burd S., 1952, ApJ 116, 8
Belopolsky A., 1914, Astron. Nachr. 196, 1
Borra E.F., Landstreet J.D., 1977, ApJ 212, 141
Borra E.F., Vaughan A., 1978, ApJ 220, 924
Farnsworth G., 1932, ApJ 75, 364
Gerth E., Glagolevskij Yu.V., Scholz G., 1997, In: Glagolevskij Yu.V., Romanyuk I.I. (eds.) Stellar Magnetic Fields. Moscow, 67
Gerth E., Glagolevskij Yu.V., Scholz G., 1998, Contr. Astron. Obs. Skalnate Pleso 27, 455
Glagolevskij Yu.V., 1994, AZh 71, 858
Glagolevskij Yu.V., Gerth E., Hildebrandt G., Scholz G., 1998, Contr. Astrom. Obs. Skalnate Pleso 27, 461
Hildebrandt G., Woche M., Rendtel J., Scholz G., 1997, Astron. Nachr. 318, 291
Khokhlova V.L., Pavlova B.M., 1984, Pisma AZh 10, 377
Ludendorff, H., 1906, Astron. Nachr. 173, 1
Lehmann H., Scholz G., Hildebrandt G., et al., 1995, A&A 300, 783
Mégessier C., 1984, A&A 138, 267
Mathys G., Hubrig S., Landstreet J.D., Lanz T., Manfroid J., 1997, A&AS 123, 353
Michaud G., 1970, ApJ 160, 641
Oetken L., 1977, Astron. Nachr. 298, 197
Oetken L., 1979, Astron. Nachr. 300, 1
Oetken L., Bartl E., Orwert R., 1970, Astron. Nachr. 292, 1
Pyper D., 1969, ApJS 18, 347
Rufener F., 1981, A&AS 41, 207
Scholz G., Lehmann H., Harmanec P., Gerth E., Hildebrandt G., 1997a, A&A 320, 791
Scholz G., Hildebrandt G., Lehmann H., Glagolevskij Yu.V., 1997b, A&A 325, 529
Struve O., Swings P., 1943, ApJ 98, 361